DALTON
FULL PAPER

A homoleptic, self-assembled [2 × 2] square Cu_4 complex exhibiting intramolecular ferromagnetic exchange

Zhiqiang Xu, Laurence K. Thompson * and David O. Miller

Department of Chemistry, Memorial University of Newfoundland, St. John's, Newfoundland, A1B 3X7, Canada. E-mail: lthomp@mun.ca

Received 29th January 2002, Accepted 12th April 2002
First published as an Advance Article on the web 14th May 2002

A carboxylic acid-substituted picolinic hydrazone ligand (pcoap) forms a homoleptic [2 × 2] tetranuclear Cu(II)$_4$ complex with four six-coordinate Cu(II) centers bridged by μ-O alkoxide groups in a square grid structure. The terminal carboxylic groups complete the six-coordinate structures at each copper centre, capping off external coordination positions, with two functioning as carboxylates, and two in neutral carboxylic acid form. Despite very large Cu–O–Cu bridge angles (139.2–140.6°), and short Cu–Cu distances (3.97–4.05 Å), which would normally be expected to propagate antiferromagnetic exchange interactions within the grid, strictly orthogonal bridging connections between the metal centers lead to intramolecular ferromagnetic exchange (J = 7.2(3) cm^{-1}), and an S = 4/2 magnetic ground state.

Introduction

Ligands based on a picolinic hydrazide framework, *e.g.* poap (Scheme 1), have two contiguous coordination pockets juxta-

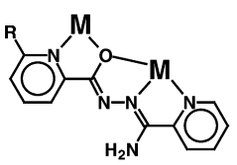

poap (R=H); epoap (R=CO_2Me); pcoap (R=COOH)

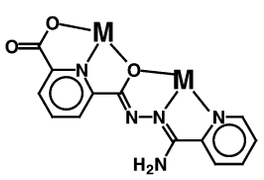

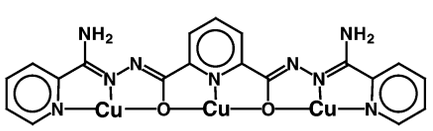

2poap

Scheme 1

posed conveniently to self assemble transition metal ions M(II) (M=Mn(II), Fe(III), Co(II), Ni(II), Cu(II), Zn(II)) into non-homoleptic homo- and hetero-tetranuclear [2 × 2] square grids, with alkoxide oxygen atoms bridging the metals in close proximity and metal–metal separations around 4 Å.[1–3] The large M–O–M bridge angles lead to antiferromagnetic exchange in the case of Mn(II), Ni(II) and Co(II) homo-tetranuclear systems, but as a result of strict magnetic orbital orthogonality within the square grids containing Cu(II), the copper systems exhibit intramolecular ferromagnetic coupling. This contrasts markedly with the report of a comparable phenoxide-bridged [2 × 2] Cu(II) square grid with orthogonal bridging connections, which was shown to exhibit weak intramolecular antiferromagentic coupling.[4]

Each ligand, *e.g.* poap, provides four donor atoms and fills five metal ion coordination positions. As a consequence, for six-coordinate metal ions, four additional ligands are required at external coordination positions (Scheme 1). These are usually solvent (*e.g.* water molecules) or anions (*e.g.* NO_3^-). In order to encapsulate the four-metal grid in a homoleptic arrangement of ligands, one additional coordination site per metal needs to be satisfied by a suitably positioned ligand donor group. The ligand pcoap (Scheme 1) has a carboxylic acid group at the pyridine 6-position, and would form an additional five-membered chelate ring, thus extending the two coordination pockets to include five donor atoms (Scheme 1). The synthesis of this unusual unsymmetric ligand will be described, based on the differing solubilities of mono- and di-substituted intermediates (Scheme 2), and its [2 × 2] homoleptic square Cu(II)$_4$ complex discussed. The related fully di-substituted ligand 2poap (Scheme 1) is tritopic in nature, and self-assembles to produce novel square [3 × 3] M_9 grids.[5–9]

Experimental

Physical measurements

Infrared spectra were recorded from Nujol mulls using a Mattson Polaris FT-IR instrument. Microanalyses were carried out by Canadian Microanalytical Service, Delta, Canada. UV/vis spectra were collected from dispersed mulls using a Cary 5E spectrometer. Mass spectra were obtained using a VG Micromass 7070HS spectrometer. Variable temperature magnetic data (2–300 K) were obtained using a Quantum Design MPMS5S SQUID magnetometer with field strengths in the range 0.1 to 5.0 T. Samples were prepared in aluminium pans, and mounted inside straws for attachment to the sample transport rod. Background corrections for the sample holder assembly and diamagnetic components of the complexes were applied.

 DOI: 10.1039/b201076n

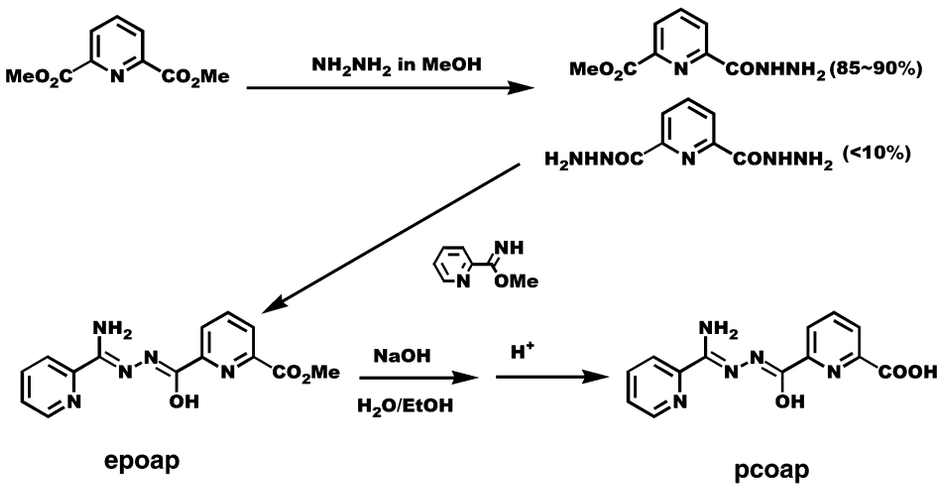

Scheme 2

Synthesis of pcoap (Scheme 2)

6-Methyloxycarbonyl-2-pyridinecarboxylic acid hydrazide. Anhydrous hydrazine (98%, 3.27 g, 0.100 mol in 150 mL methanol) was added dropwise to a stirred warm solution of dimethyl-2,6-pyridinedicarboxylate (19.8 g; 0.102 mol in 500 mL methanol) over a period of 18 h. A white crystalline solid formed during the reaction, which was filtered off, washed with methanol and dried under vacuum. This turned out to be a mixture of the major product, 6-methyloxycarbonyl-2-pyridinecarboxylic acid hydrazide (so-called mono-hydrazide), and a minor product, 2,6-pyridinedicarboxylic acid dihydrazide (so-called dihydrazide). It is possible to separate out the dihydrazide from the mixture to obtain pure mono-hydrazide by dissolving the mixture in hot water (the dihydrazide is soluble in hot water but the monohydrazide is not). However, it is more convenient to separate the byproduct after the next step in the overall reaction.

epoap. The methyl ester of iminopicolinic acid was prepared *in situ* by reaction of 2-cyanopyridine (12.6 g, 0.120 mol) with sodium methoxide solution, produced by dissolving sodium metal (0.23 g, 0.010 mmol) in dry methanol (150 mL). 7.0 g of crude 6-methyloxycarbonyl-2-pyridinecarboxylic acid hydrazide (containing a small amount of 2,6-pyridinedicarboxylic acid dihydrazide) was added to the above solution, followed by a few drops of glacial acetic acid, and the mixture was refluxed for 2 h. A light yellow powder was obtained, which was filtered off and washed with methanol. Yield: 2.58 g. This proved to be 2poap, the disubstituted iminoester condensation product (Scheme 1). 10.5 g of yellow crystals of epoap were obtained after removal of most of the solvent (methanol) and addition of about 10 mL diethyl ether. Mp: 199–201 °C. MS (*m*/*z*): 300 (M^+), 299 (M − 1), 282, 163, 107.

pcoap. 3.0 g (0.01 mol) of epoap was refluxed with a solution containing 1.0 g NaOH, 20 mL H_2O and 10 mL EtOH, for 4–5 h. The volume of the clean yellowish solution was reduced to about 15 mL, and it was allowed to cool down to room temperature and neutralized with concentrated HCl. A pale yellow precipitate was collected by filtration and washed with cold water, EtOH and diethyl ether. Yield: 1.8 g (63%). Mp: 320 °C (dec.). MS (*m*/*z*): 283 (M − 2), 267 (M − H_2O), 223, 194, 169, 105. IR (Nujol) ν_{max}/cm^{-1}: 3405 (ν OH); 3328, 3264 (ν NH_2); 2514–2613 (ν NH^+); 1702 (ν COOH); 1655 (ν C=N); 997 (py). Elemental analysis on dried sample, found: C, 47.61; H, 3.94; N, 21.93; calc. for $C_{13}H_{11}N_5O_3 \cdot 2.3H_2O$: C, 47.79; H, 4.81; N, 21.44%.

Synthesis of $[Cu_4(pcoap - H)_2(pcaop - 2H)_2](NO_3)_2 \cdot 15H_2O$ (1)

pcoap (0.29 g, 1.0 mmol) was added to a warm solution of $Cu(NO_3)_2 \cdot 6H_2O$ (0.76 g, 2.0 mmol) in 5 mL water and 5 mL methanol. The resulting mixture was stirred for a few minutes, producing a clean deep green solution, which was filtered. Green crystals formed from the filtrate after several days at room temperature. Yield: 81%. IR (Nujol) ν_{max}/cm^{-1}: 3438(w) (ν H_2O); 3340(w), 3180(w) (ν NH_2); 1696 (ν C=N); 1626 (ν COO); 1015(m) (py); 1760(w) (ν NO_3). UV/vis λ/nm: 380, 420(sh), 450(sh), 730, 920(br). Elemental analysis on vacuum dried sample, found: C, 37.01; H, 2.91; N, 18.92; calc. for $(C_{13}H_{10}N_5O_3)_2(C_{13}H_9N_5O_3)_2Cu_4(NO_3)_2(H_2O)_8$: C, 37.69; H, 3.28; N, 18.60%.

Table 1 Crystal data and structure refinement parameters for compound **1**

Empirical formula	$C_{52}H_{68}N_{22}O_{33}Cu_4$
Formula weight	1783.42
Temperature/K	190(1)
Wavelength/Å	0.71073
Crystal system	Tetragonal
Space group	$P4_3$ (no. 78)
a/Å	13.7944(7)
c/Å	40.546(4)
V/Å^3	7715.3(7)
Z	4
D_{calc}/g cm^{-3}	1.535
μ/cm^{-1}	11.58
R_1	0.090
wR_2	0.243

[a] $R_1 = \Sigma||F_o| - |F_c||/\Sigma|F_o|$, $wR_2 = \{\Sigma[w(F_o^2 - F_c^2)^2]/\Sigma[w(F_o^2)^2]\}^{1/2}$.

X-Ray crystallography

Crystallographic data and refinement of the structure. The diffraction intensities of a green prismatic crystal of **1** were collected with graphite monochromatized Mo-Kα X-radiation (rotating anode generator) using a Bruker P4/CCD diffractometer at 193(1) K to a maximum 2θ value of 52.8°. The data were corrected for Lorentz and polarization effects. The structure was solved by direct methods.[10,11] All atoms except hydrogens were refined anisotropically. Two hydrogen atoms [attached to carboxylate oxygen atoms O(9) and O(12)] were located in a difference map. Other hydrogen atoms were placed in calculated positions with isotropic thermal parameters set to 20% greater than their bonded partners, and were not refined. Neutral atom scattering factors[12] and anomalous-dispersion terms[13,14] were taken from the usual sources. All other calculations were performed with the teXsan[15] crystallographic software package using a PC.

Selected crystal data for **1** are given in Table 1.

CCDC reference number 178403.

See http://www.rsc.org/suppdata/dt/b2/b201076n/ for crystallographic data in CIF or other electronic format.

Results and discussion

Structure of $[Cu_4(pcoap - H)_2(pcaop - 2H)_2](NO_3)_2 \cdot 15H_2O$ (1)

The structure of **1** is illustrated in Fig. 1, and selected bond

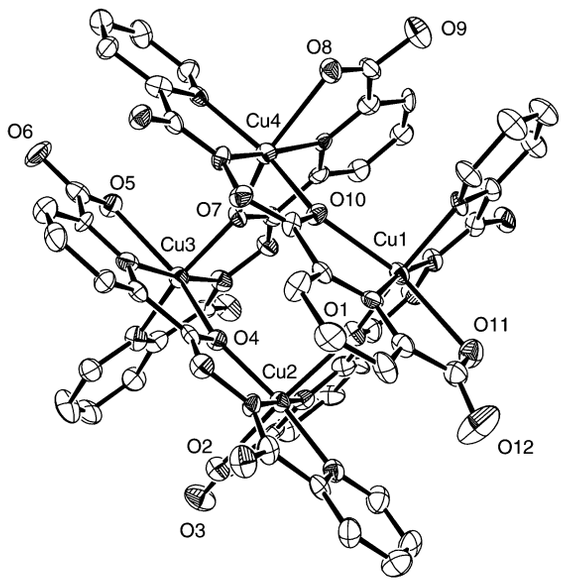

Fig. 1 Structural representation of **1** (40% thermal ellipsoids).

distances and angles are listed in Table 2. The grid consists of four six-coordinate copper centers arranged in a square, with alkoxide bridges connecting the metal atoms. Four ligands are arranged in parallel pairs in an opposed arrangement above and below the metal plane, with the carboxylate oxygen atoms filling terminal coordination positions. Cu–Cu separations fall in the range 3.97–4.05 Å, typical for systems of this sort, and Cu–O–Cu angles fall in the range 139.2–140.5°. Each copper ion is tetragonally distorted, undergoing axial elongation involving the terminal carboxylate and the bridging alkoxide oxygen atoms (Cu–O distances 2.242–2.451 Å). In-plane copper ligand contacts fall in the range 1.874–2.101 Å.

The presence of two nitrate groups in the lattice implies that the combination of four ligands provides six negative charges, and it is reasonable to assume that each ligand loses a proton from within the hydrazide framework (not the NH_2 group), leading to a negative charge on the alkoxide oxygen atom. This is supported by one relatively short Cu–O contact to each copper ion (1.995–2.025 Å) and C–O bond lengths that have substantial single bond character. In order to balance overall charge, two ligands must therefore have two negative charges, which implies that two carboxylic acid groups are deprotonated. Two protons were located in a difference map on O(9) and O(12), in agreement with this assumption.

The most prominent feature of the structure involves the encapsulation of the four six-coordinate Cu(II) centers within the grid, an unusual feature in related non-homoleptic Cu_4 [2 × 2] square grid complexes,[1–3] but similar to the phenoxide-bridged [2 × 2] copper(II) grid reported by Lehn *et al.*[4] Copper(II) undergoes Jahn–Teller distortion, and, in this case, each six-coordinate copper ion undergoes a tetragonal elongation. The axis of elongation of each copper center includes only one bridging oxygen connection, leading to a situation where the copper equatorial planes are tilted at ~90° to those of neighboring metal centers in all cases. This orbital orthogonality situation leads to a significant magnetic consequence, that of intramolecular ferromagnetic exchange (*vide infra*).

The lattice structure involves a large number of water molecules, as is typical for grids in this class,[1–3] and two significant intermolecular contacts have been identified, which might be considered to have magnetic consequences. Fig. 2 shows close contacts between carboxylate oxygen atoms O(3), O(6), O(9) and O(12) and intervening water molecules O(20), O(21), O(23) and O(35) [O(3)–O(35) 2.696; O(35)–O(21) 2.768; (O21)–O(12) 2.496; O(9)–O(23) 2.518; O(23)–O(20) 2.748; O(20)–O(6) 2.543; O(21)–O(23) 2.641 Å], forming a connected layer of grid

Table 2 Bond distances (Å) and angles (°) for **1**

N3–Cu1	1.904(11)	O7–Cu4	2.242(8)
N20–Cu1	1.983(11)	O8–Cu4	2.422(9)
O1–Cu1	2.005(8)	Cu1–Cu2	4.047(4)
N1–Cu1	2.067(9)	Cu1–Cu4	4.037(4)
O10–Cu1	2.274(8)	Cu2–Cu3	4.022(3)
O11–Cu1	2.451(11)	Cu3–Cu4	3.973(4)
N8–Cu2	1.904(11)	N3–Cu1–N20	170.5(4)
N5–Cu2	1.999(10)	N3–Cu1–O1	80.0(4)
O4–Cu2	2.004(8)	N20–Cu1–O1	98.7(3)
N6–Cu2	2.101(11)	N3–Cu1–N1	79.1(4)
O1–Cu2	2.297(8)	20–Cu1–N1	102.1(4)
O2–Cu2	2.328(10)	O1–Cu1–N1	159.1(3)
N13–Cu3	1.909(11)	N3–Cu1–O10	113.0(4)
O7–Cu3	1.995(8)	N20–Cu1–O10	76.5(4)
N10–Cu3	2.026(11)	O1–Cu1–O10	94.8(3)
N11–Cu3	2.046(11)	N1–Cu1–O10	92.8(3)
O4–Cu3	2.281(8)	N8–Cu2–N5	176.9(5)
O5–Cu3	2.428(8)	N8–Cu2–O4	79.3(4)
N18–Cu4	1.874(10)	N5–Cu2–O4	99.3(4)
N15–Cu4	2.005(9)	N8–Cu2–N6	77.9(4)
O10–Cu4	2.025(8)	N5–Cu2–N6	103.4(4)
N16–Cu4	2.056(10)	O4–Cu2–N6	157.2(4)
N8–Cu2–O1	107.7(4)	N11–Cu3–O5	91.6(4)
N5–Cu2–O1	75.0(4)	O4–Cu3–O5	150.9(3)
O4–Cu2–O1	93.1(3)	N18–Cu4–N15	169.4(4)
N6–Cu2–O1	95.1(3)	N18–Cu4–O10	79.3(4)
N8–Cu2–O2	100.7(4)	N15–Cu4–O10	96.4(4)
N5–Cu2–O2	76.6(4)	N18–Cu4–N16	79.8(4)
O4–Cu2–O2	90.9(3)	N15–Cu4–N16	104.5(4)
N6–Cu2–O2	91.9(4)	O10–Cu4–N16	159.0(3)
O1–Cu2–O2	151.6(3)	N18–Cu4–O7	113.7(4)
N13–Cu3–O7	79.9(4)	N15–Cu4–O7	76.1(3)
N13–Cu3–N10	172.0(5)	O10–Cu4–O7	95.0(3)
O7–Cu3–N10	96.7(4)	N16–Cu4–O7	92.4(3)
N13–Cu3–N11	78.7(4)	N18–Cu4–O8	95.8(4)
O7–Cu3–N11	158.6(4)	N15–Cu4–O8	74.6(4)
N10–Cu3–N11	104.4(4)	O10–Cu4–O8	91.7(3)
N13–Cu3–O4	110.6(4)	N16–Cu4–O8	91.4(3)
O7–Cu3–O4	92.9(3)	O7–Cu4–O8	150.5(3)
N10–Cu3–O4	76.6(4)	Cu1–O1–Cu2	139.5(4)
N11–Cu3–O4	95.5(3)	Cu2–O4–Cu3	139.6(4)
N13–Cu3–O5	98.4(4)	Cu3–O7–Cu4	139.2(4)
O7–Cu3–O5	90.4(3)	Cu4–O10–Cu1	140.5(4)
N10–Cu3–O5	74.4(4)		

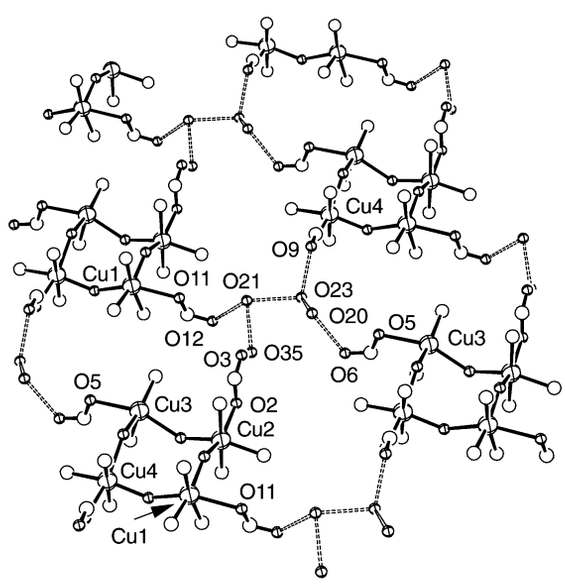

Fig. 2 Structural representation of lattice contacts between Cu_4 grid subunits.

molecules in the *xy* plane. These contacts are within reasonable hydrogen bonding distances, and could provide long intermolecular magnetic exchange pathways between Cu_4 grids (*vide infra*).

Magnetic properties

Variable temperature magnetic data (μ_{mol}) for **1** measured at 0.1 T are shown in Fig. 3. The room temperature magnetic

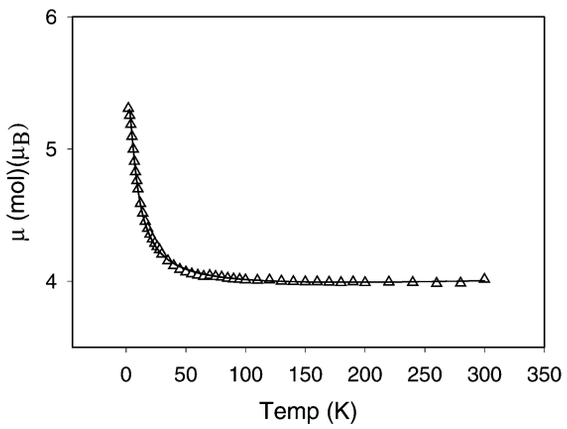

Fig. 3 Variable temperature magnetism of **1** (μ_{mol}). The solid line represents the best data fit with g = 2.246(7), J = 7.2(3) cm^{-1}, TIP = 250 × 10^{-6} emu mol^{-1} and θ = −0.15 K {10^2R = 0.58; R = $[\Sigma (\chi_{obs} - \chi_{calc})^2/\Sigma \chi_{obs}^2]^{1/2}$).

moment is 4.01 μ_B and as temperature is lowered, the value gradually increases, reaching 5.31 μ_B at 2 K. This behavior is indicative of the presence of dominant intramolecular ferromagnetic exchange. The variable temperature data were fitted to an isotropic exchange expression derived from the exchange Hamiltonian (eqn. 1), which assumes a single exchange integral within the square grid.

$$\mathbf{H} = -J\{\boldsymbol{S}_1\cdot\boldsymbol{S}_2 + \boldsymbol{S}_2\cdot\boldsymbol{S}_3 + \boldsymbol{S}_3\cdot\boldsymbol{S}_4 + \boldsymbol{S}_1\cdot\boldsymbol{S}_4\} \qquad (1)$$

The total spin-state combinations, and their energies, were calculated in the normal way using the Kambe approach,[16] and substituted into the van Vleck equation to generate the appropriate exchange expression. This was achieved within the software of the MAGMUN4.0 magnetic package.[17] The experimental data were fitted successfully to the derived magnetic model (based on eqn. 1), within MAGMUN4.0, to give g = 2.246(7), J = 7.2(3) cm^{-1}, ρ = 0, TIP = 250 × 10^{-6} emu mol^{-1} and θ = −0.15 K (ρ is the fraction of paramagnetic impurity, TIP is temperature independent paramagnetism and θ is a Weiss-like correction indicative of possible intermolecular exchange) {10^2R = 0.58; R = $[\Sigma (\chi_{obs} - \chi_{calc})^2/\Sigma \chi_{obs}^2]^{1/2}$}. The solid line in Fig. 3 was calculated with these parameters. Many regression analyses were carried out over an extended range of variables and, in all cases, a small negative θ value was required in order to optimize the fitting. This suggests the presence of a weak intermolecular exchange effect which is antiferromagnetic in nature. This is tentatively assigned to the close contacts between grid subunits and water molecules, as described previously.

Confirmation of the expected S = 4/2 ground state was obtained by measuring magnetization as a function of field at 2 K (Fig. 4). The magnetization data were fitted successfully to the appropriate Brillouin function with g = 2.258, very close to the value obtained from the variable temperature analysis (the solid line in Fig. 4 represents the best fit). This result is entirely consistent with those reported previously for related Cu_4 square grids,[1–3] and is in agreement with the strictly orthogonal bridging arrangement between adjacent copper magnetic orbitals in the structure, and the close proximity of the copper(II) centers.

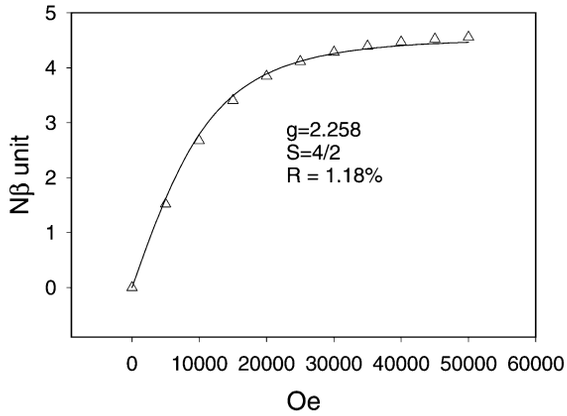

Fig. 4 Magnetization *versus* field data for **1** at 2 K. The solid line represents the best fit to the theoretical Brillouin function for S = 4/2, g = 2.258.

This is remarkable in the sense that the large Cu–O–Cu bridge angles would have normally been expected to propagate strong antiferromagentic exchange had the magnetic copper orbitals been directly involved in oxygen overlap in a bridging arrangement, as is the case for essentially planar tetranuclear $Cu_4(\mu\text{-}O)_4$ complexes with the metal ions constrained within a macrocyclic ligand framework.[18–20] The extra organizational freedom that results from the self assembly reaction with the alkoxyamidrazone ligands in this class allows the metal ions to adopt a different, and perhaps preferred, arrangement, with novel orthogonal bridging connections.

Conclusion

Compound **1** represents the first example of a ferromagnetic, homoleptic square [2 × 2] grid with ligands of this type, and introduces a useful reactive appendage on the ligand, which can be further functionalized and used as a potential tether group for possible surface applications. The ligand synthesis is possible as a result of the differing solubilities of intermediates in the reaction sequence, and it is of relevance to note that the fully functionalized ligand 2poap, which has a second appended amidrazone group (Scheme 1) forms [3 × 3] M_9 magnetic grids.[5–9]

Acknowledgements

We thank NSERC (Natural Sciences and Engineering Research Council of Canada) for financial support, and Dr M. J. Ferguson, University of Alberta, for X-ray structural data.

References

1 C. J. Matthews, K. Avery, Z. Xu, L. K. Thompson, L. Zhao, D. O. Miller, K. Biradha, K. Poirier, M. J. Zaworotko, C. Wilson, A. E. Goeta and J. A. K. Howard, *Inorg. Chem.*, 1999, **38**, 5266.
2 Z. Xu, L. K. Thompson, C. J. Matthews, D. O. Miller, A. E. Goeta and J. A. K. Howard, *Inorg. Chem.*, 2001, **40**, 2446.
3 L. K. Thompson, C. J. Matthews, L. Zhao, Z. Xu, D. O. Miller, C. Wilson, M. A. Leech, J. A. K. Howard, S. L. Heath, A. G. Whittaker and R. E. P. Winpenny, *J. Solid State Chem.*, 2001, **159**, 308.
4 T. Rojo, J.-M. Lehn, G. Baum, D. Fenske, O. Waldmann and P. Müller, *Eur. J. Inorg. Chem.*, 1999, 517.
5 L. Zhao, Z. Xu, L. K. Thompson and D. O. Miller, *Polyhedron*, 2001, **20**, 1359.
6 L. Zhao, Z. Xu, L. K. Thompson, S. L. Heath, D. O. Miller and M. Ohba, *Angew. Chem., Int. Ed.*, 2000, **39**, 3114.
7 L. Zhao, C. J. Matthews, L. K. Thompson and S. L. Heath, *Chem. Commun.*, 2000, 265.
8 O. Waldmann, R. Koch, S. Schromm, P. Müller, L. Zhao and L. K. Thompson, *Chem. Phys. Lett.*, 2000, **332**, 73.

9 O. Waldmann, L. Zhao and L. K. Thompson, *Phys. Rev. Lett.*, 2002, **88**, 66401.
10 (*a*) G. M. Sheldrick, SHELX97, University of Göttingen, Germany, 1997; (*b*) SIR97: A. Altomare, M. Cascarano, C. Giacovazzo and A. Guagliardi, *J. Appl. Crystallogr.*, 1993, **26**, 343.
11 P. T. Beurskens, G. Admiraal, G. Beurskens, W. P. Bosman, R. de Gelder, R. Israel and J. M. M. Smits, *The DIRDIF-94 Program System, Technical Report of the Crystallography Laboratory*, University of Nijmegen, The Netherlands, 1994.
12 D. T. Cromer and J. T. Waber, *International Tables for X-ray Crystallography*, The Kynoch Press, Birmingham, 1974, vol. IV, Table 2.2A.
13 J. A. Ibers and W. C. Hamilton, *Acta Crystallogr.*, 1964, **17**, 781.
14 D. C. Creagh and W. J. McAuley, *International Tables for Crystallography*, ed. A. J. C. Wilson, Kluwer Academic Publishers, Boston, MA, 1992, vol. C, pp. 219–222, Table 4.2.6.8,.
15 *teXsan for Windows*, Crystal Structure Analysis Package, Molecular Structure Corporation, The Woodlands, TX, 1997.
16 K. Kambe, *J. Phys. Soc. Jpn.*, 1950, **5**, 38.
17 Z. Xu, K. He, L. K. Thompson and O. Waldmann, MAGMUN4. 0, Memorial University of Newfoundland, St. John's, NF, Canada, 2002.
18 V. McKee and S. S. Tandon, *J. Chem. Soc., Chem. Commun.*, 1988, 385.
19 V. McKee and S. S. Tandon, *Inorg. Chem.*, 1989, **28**, 2902.
20 V. McKee and S. S. Tandon, *J. Chem. Soc., Dalton Trans.*, 1991, 221.